VOLCANISM WITHIN FLOOR-FRACTURED ATLAS CRATER. L. Gaddis[1], B.R. Hawke[2], T. Giguere[2,3], S. Klem[1], J.O.Gustafson[4], S.J. Lawrence[5], and J.D. Stopar[5]. [1]Astrogeology Science Center, U.S. Geological Survey, Flagstaff, AZ; [2]Univ. Hawaii, Honolulu, HI; [3]Intergraph Corp., P.O. Box 75330, Kapolei, HI; [4]Dept. Earth & Atmospheric Sciences, Cornell University, Ithaca, NY; [5]School of Earth and Space Exploration, Arizona State University, Tempe, AZ. (lgaddis@usgs.gov).

Introduction: Recent observations of the lunar floor-fractured crater Atlas (46.7°N, 44.4°E, 87 km dia.) by imaging instruments on the Lunar Reconnaissance Orbiter (LRO) and SELENE/Kaguya missions [1, 2, 3] allow us to examine in detail two small pyroclastic volcanic deposits in the crater floor. We used data from the Kaguya Terrain Camera (TC; ~10 m/pixel) and Multiband Imager (MI; 5 visible wavelength or VIS channels at 415 to 1000 nm, ~20 m/pixel), and from the Narrow Angle Camera (NAC; 0.5 to 2.0 m/pixel) subsystem of the LRO Camera. We characterize deposit surface textures, their spatial distribution and thickness, and their likely source vents.

Lunar pyroclastic deposits are of interest in part because they are thought to be volatile- and metallic-element (e.g., S, Fe, Ti) enriched remnants of ancient lunar volcanic eruptions. Their compositions and distributions provide information on the early lunar interior [4-7] and the distribution of possible resource materials [8, 9]. Studies of pyroclastic deposits with telescopic and Clementine color (ultraviolet, visible or UVVIS) data demonstrated their compositional heterogeneity and expanded our knowledge of deposit types [11-16]. Lunar pyroclastic deposits tend to be very dark, with smooth surface textures [e.g., 9, 11, 12]; the smaller or localized deposits are typically <1000 km^2 and are associated with endogenic craters or irregular depressions.

Atlas Pyroclastics: Two small pyroclastic deposits have been identified in the floor of the Upper Imbrian Atlas crater [13], associated with northern (N) and southern (S) vents (*Figure 1*). The N deposit was thought to be smaller (~100 km^2) than the S deposit (~250 km^2) [14], and both were believed to have been emplaced by explosive, vulcanian-style eruptions [17]. Spectra of both Atlas pyroclastic deposits indicate the presence of feldspar-bearing mafic minerals dominated by orthopyroxene. Although resembling highlands compositions, these deposits may also contain clinopyroxene, glass, and/or olivine [13].

Analyses of MI VIS and NAC data confirm that both the N and S deposits are associated with fractures that ring the crater floor. In both areas, wider segments of floor fractures were previously identified as source vents, and this is supported by deposit distribution (*Figures 2, 3*) and topographic relief [GLD100, 18]. Although many portions of the crater floor have dark deposits, no other vents are apparent. The major N-S trending floor fracture (~1.2 km average width) appears unmantled except near the pyroclastic vents.

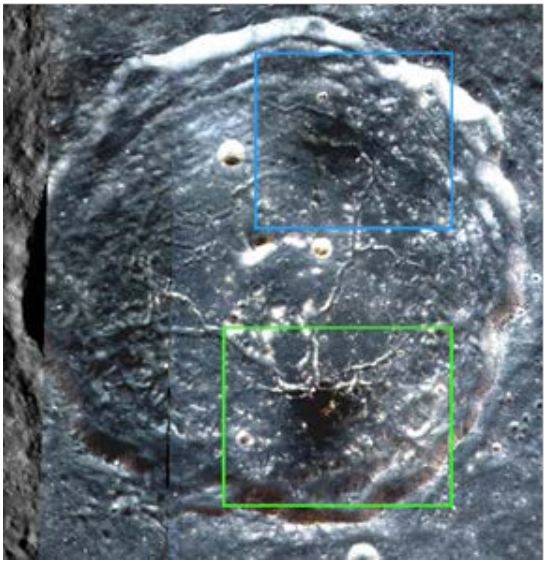

Figure 1. MI color composite mosaic of Atlas crater (87 km dia.), (VIS bands, red=3, green=2, blue=1) on TC evening mosaic. Northern vent and deposit are outlined in blue; southern vent and deposits are outlined in green.

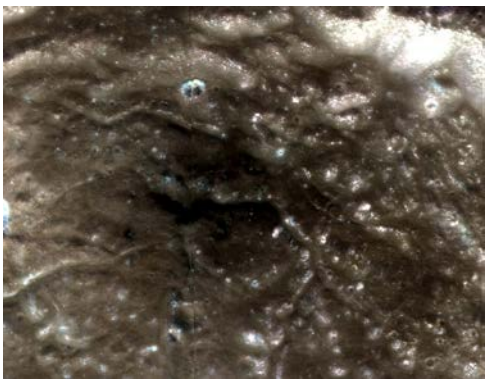

Figure 2. MI color composite mosaic of northern vent and pyroclastic deposit in Atlas crater (VIS bands, red=3, green=2, blue=1). Image is 35 km across, North is toward the top.

The N deposit (*Figure 2*) is dark, boulder-free, and irregularly shaped (~19.5 km X ~25.4 km), distributed around an E-W trending elongate fracture (~2.0 km X 9.5 km) and a smaller irregular

depression (~2.3 km X 7.2 km, 3.3 km depth). Small crater diameters and their penetration depths [e.g., 19] indicate deposit thicknesses of 0.5 to 6.0 m. The S deposit (*Figure 3*) appears darker, boulder-free, and more symmetrically distributed (~12.6 km X ~15.8 km) around a SW-NE trending irregular depression (~7.7 km X 12.7 km, 3.5 km depth). Deposit thickness varies between 0.5 m distally to 5 m near the vent. NAC data for more distal areas of the southern deposit (*Figure 4*) show that segments of fracture walls within the southern deposit are mantled with smooth, very dark material that has adhered to ~steep slopes and may have been somewhat plastic when emplaced. Tracks from occasional meter-sized boulders from fracture walls are observed on the dark mantle.

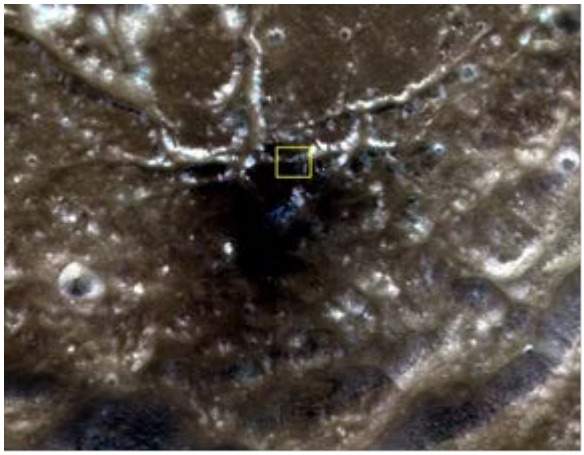

Figure 3. MI color composite mosaic of southern vent and pyroclastic deposit in Atlas crater (VIS bands, red=3, green=2, blue=1). Image is 40 km across, North is toward the top. Yellow box marks location of Figure 4 image.

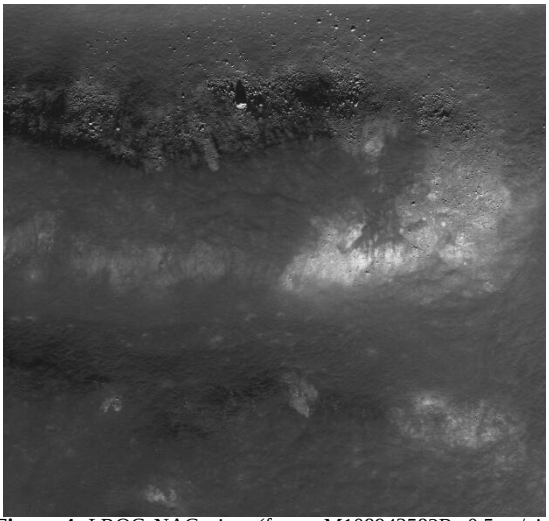

Figure 4. LROC NAC view (frame M108943582R, 0.5 m/pixel, 48° inc.) of mantled fracture on south floor of Atlas crater (yellow box, Figure 3; image is ~1.6 km across).

MI-VIS spectra for Atlas deposits indicate that the floor of the crater is composed of fractured material of highlands composition; wall units and high-albedo knobs of fracture outcrops resemble fresh craters. Mature soil of highlands composition overlies much of the crater floor. The pyroclastic deposits are dark, have absorption bands centered near 900 nm, and resemble the orthopyroxene-rich materials typical of "Group 1" small pyroclastic deposits [13].

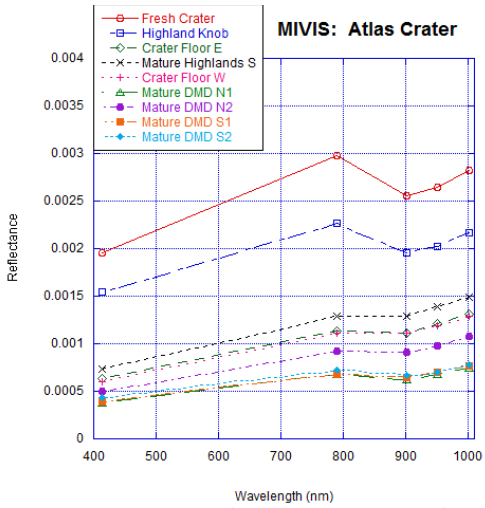

Figure 5. MI VIS spectra of Atlas crater units. Reflectance is derived using data for the calibration site at Apollo 16 [after 3].

Summary: Two localized pyroclastic deposits and their vents are observed in the floor of Atlas crater. Both deposits appear to represent low-volume eruptions of pyroclastic material from elongate fractures or fissure vents. The northern deposit is larger than previously recognized. The possibly plastic nature of both mantling deposits suggests a more fluidized, perhaps hotter magma than is typically associated with small pyroclastic deposits.

References: [1] Robinson et al., 2010, Space Sci. Rev. 150, 81-124. [2] Haruyama et al., 2008, Adv. Sp. Res. 42, 310-316. [3] Ohtake et al., 2010, Space Sci. Rev. 154, 57-77. [4] Gaddis et al., 2009, LRO Sci. Targ. Mtg., #6025. [5] Gaddis et al., 2010, LPSC 41st, abs. #2059; [6] Heiken et al. 1974, GCA 38, 1703. [7] Delano, 1986, JGR 91, D201. [8] Shearer et al., 2006, RMG 60, 365. [9] Hawke et al., 1990, PLPSC 20th, 249. [10] Duke et al., 2006, RMG 60, 597. [11] Pieters et al., 1973, JGR 78, 5867. [12] Gaddis et al., 1985, Icarus 61, 461. [13] Hawke et al., 1989, PLPSC 19th, 255. [14] Gaddis et al., 2003, Icarus 161, 262. [15] Lucey et al., 2006, RMG 60, 83. [16] Wilcox et al., 2006, JGR 111, E09001. [17] Head and Wilson, 1979, PLPSC 10th, 2861. [18] Scholten et al., 2011, LPS 42nd, abs. #2046 and manuscript in press. [19] Melosh and Ivanov, 1999, Ann. Rev. Earth Planet. Sci. 27, 385-415.